JOURNAL OF COMPUTATIONAL PHYSICS 81, 406–420 (1989)

Solution of a Problem in the Theory of Laser Medicine by the Method of Lines

MICHAEL DAVIS, PHIROZE KAPADIA, AND PAUL WHITING

Department of Physics, University of Essex, United Kingdom

AND

JOHN DOWDEN*

Department of Mathematics, University of Essex, United Kingdom

Received October 26, 1987; revised May 31, 1988

In recent years laser power transmitted through an optical fibre has been used to provide the energy source for the treatment of tumours by local hyperthermia. The radiation from the fibre tip is scattered and absorbed by the tissue, where it is converted into thermal energy. When the tissue has been raised above about 43 °C for a length of time depending on the temperature, it dies; at the same time the removal of energy by perfusion of the blood supply also ceases. The method is restricted in the volume that can be treated using a single fibre, so fibre clusters are now being introduced. A computer program has been written which solves the equations governing both the scattering and absorption processes and the heat conduction problem, using the method of lines. Computed results have been found which agree qualitatively with the limited amount of evidence at present available and is here demonstrated for the case of a cluster of five fibres. With accurate values of the physical parameters, computations such as these can be a useful additional guide to the surgeon when making decisions about method of treatment, location, and exposure time.

1. THE MATHEMATICAL MODEL

A laser beam can be used to provide a very accurate beam of electromagnetic energy. This is converted into thermal energy when it interacts with tissue, and the damage caused by the resultant heating, if properly directed and controlled, is the basis of treatment of tumours by hyperthermia. Scattering as well as absorption takes place and both effects depend on the particular choice of wavelength. The kind of laser used will, therefore, be chosen for its suitability for the intended application [1]. This method differs from much laser surgery currently in use,

* Please address communications to Dr. J. M. Dowden, Department of Mathematics, University of Essex, Colchester CO4 3SQ, U.K.

0021-9991/89 $3.00

which relies on the energy of the laser to destroy and remove the tumour. With local hyperthermia however, the tissue is killed, but the body's own mechanisms are used to remove necrotic tissue, which is replaced by scar tissue or, in some cases, regenerated healthy tissue.

If only one fibre is used to treat a substantial volume, rather large temperature rises can occur at the tip. For example, a Nd-YAG laser run much in excess of the equivalent of a continuous output of 1 W produces charring at this point, and an increase in power does not appear to produce an increase in the volume treated [2]. A number of different techniques are available to overcome this problem. The exposure time can be increased, although this may lead to excessive length of treatment, and it is not yet clear how large a volume can be treated this way. Alternatively, repeated treatment with a single fibre can be used with the tip in a different position after each exposure. This is time-consuming and might lead to excessive mechanical damage. Another way is to use a stripped fibre whose end has been specially etched so that it acts more like a line source than a point source [3]. Consequently, there is less risk of charring when higher powers are used. The final possibility is to use a cluster of fibres with a suitable spacing, all energised at the same time. A much larger region can be treated this way in a single exposure even though the power transmitted down each fibre separately must not exceed the maximum value permissible when a single fibre is used in isolation. As an example of this type of treatment, this paper studies the theoretical modelling and numerical solution of this problem for a cluster of five fibres with parallel axes and coplanar tips arranged at the corners and the centre of a square.

Laser radiation is scattered as well as absorbed by the tissue through which it passes. To solve the problem accurately therefore requires solution of the transport equation [4, Chap. 7]. The complexity of this equation is such as to make it unattractive, and the diffusion approximation to that equation is used here [4, Chap. 9]. The only disadvantage of this approach is that when there is very strong absorption as well as scattering, as may be the case in the liver for example, the diffusion approximation may not be entirely appropriate. Unfortunately there does not seem to be a practical alternative at present. If the average diffused intensity passing through a particular point in whatever direction is U (W cm^{-2}), the equation satisfied by U is

$$\nabla^2 U - 3k_a k_{tr} U = -3k_s k_{tr} L, \tag{1}$$

where ∇^2 is the Laplacian operator, k_a (cm^{-1}) is an absorption coefficient, k_s (cm^{-1}) is a scattering coefficient,

$$k_t = k_a + k_s \qquad \text{and} \qquad k_{tr} = k_a + k_s(1-g);$$

g is the mean cosine of the scattering angle [5], so k_{tr} is equal to k_t when the scatterers are isotropic. The quantity L (W cm^{-2}) is the sum of all terms due to incident radiation from the laser beam. For a single axially symmetric point source

with a uniform power distribution in a cone of angle α about the axis, the form of L at a distance r from the source is

$$L(s) = \begin{cases} K \exp(-k_t s)/(4\pi r \sin \tfrac{1}{2}\alpha)^2, & \text{inside the cone} \\ 0, & \text{outside the cone,} \end{cases}$$

where the total power being delivered is K (W). In the problem studied numerically here there are five identical such sources each of which have values for K which are uniform inside, and zero outside, a cone centred in the forward direction on the axis of the optical fibres with an angle α from the axis.

The temperature distribution T (°C) is then governed by a form of the bio-heat equation

$$\rho c \frac{\partial}{\partial t}(T - T_0) = \nabla \cdot \lambda \nabla (T - T_0) + 4\pi k_a (L + U) - \begin{cases} q \rho_b c_b (T - T_0) & \text{(live tissue)} \\ 0 & \text{(dead tissue).} \end{cases} \tag{2}$$

Here ρ (g cm^{-3}) and ρ_b (g cm^{-3}) are the densities of the tissue and of blood, respectively, while c (J g^{-1} °C^{-1}) and c_b (J g^{-1} °C^{-1}) are their respective specific heats; q (s^{-1}) is the perfusion rate; T_0 is body temperature; and λ (J cm^{-1} s^{-1} °C^{-1}) is the thermal conductivity of the tissue. The values of these parameters are close to those for water although some of them are temperature dependent to some extent; q, for example, depends on the rate of metabolism and hence depends on van 't Hoff's equation [6] while the optical constants can vary considerably during the course of treatment at least when the power from a single fibre of 400 μm diameter is above 1.5 W [2]. The variations can be caused by dehydration, tissue shrinkage, deoxygenation of haemoglobin, or destruction of morphological structure, as well as temperature dependence. These effects, however, have not been included here as the former is probably not important for the exposure times considered and the latter is not yet properly quantified.

The final problem is to determine whether the tissue is alive or dead; although the solution of the problem does itself depend on this, it is the final form of this region which is of interest to the surgeon. He is interested in knowing that he has affected a region in which no malignant cell will survive to produce further malignant cells. The exact cause of the death of tissue is to some extent irrelevant and may be the indirect result of coagulation or irreversible vascular constriction or direct physical damage to the cell itself. Whatever the immediate cause, necrosis depends on exposure for a minimum length of time to a temperature above T_0. There appears to be a minimum value, $T_{\min}$, for which this will occur [2] which seems to be about 42.5 °C. For temperatures above $T_{\min}$ it is known empirically that the exposure necessary halves with each degree rise in temperature, if the tissue is held at a fixed temperature for the given time [7]. When the temperature varies with time a more sophisticated test must be used, for example, an "ageing function"

[8] or "damage integral" [9]. Over the small range of temperatures relevant here, the two approaches are essentially equivalent. We shall adopt the first approach here. If tissue dies after a time $\tau(T)$ (s) when it is exposed to a uniform constant temperature T, then even if the temperature is varying the tissue is assumed to die after the length of time at which

$$\int_{T>T_{\min}}^{t} \frac{dt}{\tau(T)} = 1. \tag{3}$$

We shall take

$$\tau(T) = (\tfrac{1}{2})^{T-T_0-9}\tau(46),$$

where T_0 is 37 °C and $\tau(46)$ is a convenient reference value; notice that when T is 46 °C this is an identity. A substantial problem is that no accurate values of τ are known. The most complete set of experiments reported so far were on pig-skin [9] and suggest that $\tau(46)$ may be an hour. On the other hand, this value does not really seem to be consistent with Matthewson's experiments [2] which suggest values that are much shorter; considering the large number of effects to be taken into account in these experiments, which were performed on the livers of live rats, it is not at all easy to estimate this parameter. There is, however, no particular reason to suppose that it is the same for different tissues or that it is appropriate over the whole of the temperature range. Below about 42.5 °C, $\tau(T)$ is effectively infinite and above about 60 °C coagulation occurs rapidly. As this is a somewhat different mechanism leading to cell death, τ is unlikely to be given by the same rule. Further, on careful inspection, Matthewson's results [2] suggest that this rule is only approximately true for rats' livers and that there is a change in it somewhere in the region of 48–50 °C; this is also a possible interpretation of some of the results reported by Dickson and Calderwood [7]. There is sometimes a problem of long-term accurate positioning of the tips of the fibres in living tissue which may be in substantial motion; this is true of the liver, for example. It can be avoided by using treatment times of the order of only a few minutes, so that the very long time-scales of the conventional hyperthermia range, in the low 40's, are not too important, and the exact time-scales of the rapid cell death at temperatures over the low 50's are not important. The most significant temperatures would seem to be 45–55 °C, and an accurate knowledge of $\tau(T)$ for this range is important. The rule given here seems to be widely accepted, at least in the lower part of the range (Dickson and Calderwood [7]) and a value for $\tau(46)$ of about 15 min is compatible with a wide range of results; see [7], although an accurate evaluation of the rule specifically for the liver is not yet available.

Special solutions of Eqs. (1) and (2) can be found in the limit as $t \to \infty$. In particular, the distinction between live and dead tissue can be ignored in Eq. (2), so that either q is taken as constant and non-zero everywhere, or zero everywhere. In either case, spherically symmetric solutions of these equations can be obtained in closed analytical form for the equilibrium temperature distribution attained after

a long period of time. The necrotic zone is then obtained from (3) very simply as a slowly increasing function of time for a single point source. For multiple sources, the temperature distribution can be obtained by linear superposition before (3) is used to calculate the necrotic zone.

The spherically symmetric equilibrium solution ($\alpha = \pi$) used for this purpose has the following form. If s is the distance from the source to the point at which U and T are required then they can be expressed in terms of dimensionless functions u and f by writing

$$U = \frac{k_0 k_s K}{32\pi^2} \left\{\frac{3k_{tr}}{k_a}\right\}^{1/2} u(s, k_0, k_t),$$

where

$$k_0 = (3k_a k_{tr})^{1/2}$$

and

$$u(r, k_0, k_t) = \left\{e^{k_0 r} E_1[(k_t + k_0)r] - e^{-k_0 r} E_1[(k_t - k_0)r] + e^{-k_0 r} \ln \frac{k_t + k_0}{|k_t - k_0|}\right\} \Big/ k_0 r.$$

Similarly,

$$T = T_0 + \frac{Kk_t}{4\pi\lambda} f(r, k_0, k_t, k_a, k_q),$$

where

$$k_q = (q\rho_b c_b/\lambda)^{1/2}$$

and

$$\begin{aligned} f(r, k_0, k_t, k_a, k_q) = {} & \left\{e^{-k_q r} \ln \frac{k_t + k_q}{|k_t - k_q|} + e^{k_q r} E_1[(k_t + k_q)r] \right. \\ & \left. - e^{-k_q r} E_1[(k_t - k_q)r]\right\} \frac{k_a}{2k_q k_t r} \\ & + \frac{(k_t - k_a)}{2(k_0^2 - k_q^2)r} \cdot \frac{k_0}{k_t} \left[e^{-k_0 r} \ln \frac{|k_0 - k_t|}{k_0 + k_t} \right. \\ & - \frac{1}{2k_q} \left\{(k_0 - k_q)\{e^{-k_0 r} E_1[(k_t - k_0)r] - e^{k_0 r} E_1[(k_t + k_0)r] \right. \\ & + e^{-k_q r} E_1[(k_t - k_q)r] - e^{k_q r} E_1[(k_t + k_q)r]\} \\ & - (k_0 + k_q)\{e^{-k_0 r} E_1[(k_t - k_0)r] - e^{k_0 r} E_1[(k_t + k_0)r] \\ & - e^{-k_q r} E_1[(k_t - k_q)r] + e^{k_q r} E_1[(k_t + k_q)r]\} \\ & \left. \left. - 2k_0 e^{-k_q r} \ln \frac{k_t + k_q}{|k_t - k_q|}\right\}\right]. \end{aligned}$$

This last expression simplifies when perfusion is ignored to give

$$f_0(r) \equiv f(r, k_0, k_t, k_a, 0)$$
$$= k_a \left\{ E_1(k_t r) + \frac{1 - e^{-k_t r}}{k_t r} \right\} \Big/ k_t + \frac{k_t - k_a}{2k_0 k_t r} \left\{ e^{-k_0 r} \ln \frac{|k_t - k_0|}{k_t + k_0} + \frac{2k_0}{k_t} (1 - e^{-k_t r}) \right.$$
$$\left. + 2k_0 r E_1(k_t r) - e^{k_0 r} E_1[(k_0 + k_t) r] + e^{-k_0 r} E_1[(k_t - k_0) r] \right\}.$$

In these expressions k_0 and k_q are measured in units of cm^{-1} and E_1 is the exponential integral

$$E_1(x) = \int_x^\infty \frac{e^{-t}}{t} dt.$$

For negative values of its argument in the foregoing expressions the Cauchy principal value must be taken, so that $E_1(x)$ should be interpreted as $-E_i(-x)$ when $x < 0$; see Abramowitz and Stegun [10]. The boundary conditions needed to obtain these solutions are

$$ru, rf \to 0 \quad \text{as} \quad r \to 0$$
$$u, f \to 0 \quad \text{as} \quad r \to \infty.$$

The equations both possess solutions in which the conditions stated as r tends to zero do not hold; those solutions correspond to spontaneous internal point sources of optical intensity and heat, respectively. Since all power comes from the laser beam ru and rf must vanish at the origin of r. Similarly, there is no input of heat or optical intensity far from the fibre tips, so that u and f must tend to zero at infinity.

This solution is applied as $t \to \infty$; the full time-independent solution would be extremely complicated in form, but simplifying assumptions permit solutions which give information about the rate at which the steady state is reached. If k_q is set equal to zero, so that perfusion is ignored, the time-dependent solution predicts a period of about a day for the temperature distribution to lie within 5% of the equilibrium value at 1 cm from the fibre tip, so that in this case the equilibrium solution is a poor guide. However, a typical value for the perfusion rate in liver is 12 ml/100 g/min and corresponds to a value for k_q of about 1 cm^{-1}. With this value, the equilibrium temperature for a given power input is substantially lower and is achieved to the same level in $7\frac{3}{4}$ min.

The equilibrium solutions can be used to investigate the nature of the dependence of the solutions on the values of such physical parameters as the scattering and absorption coefficients. Figure 1 shows some comparisons for spherically symmetric emissions from a single point source. The lower pair of curves, marked A, correspond to a perfusion rate for which $k_q = 1$ and the upper pair, B, correspond

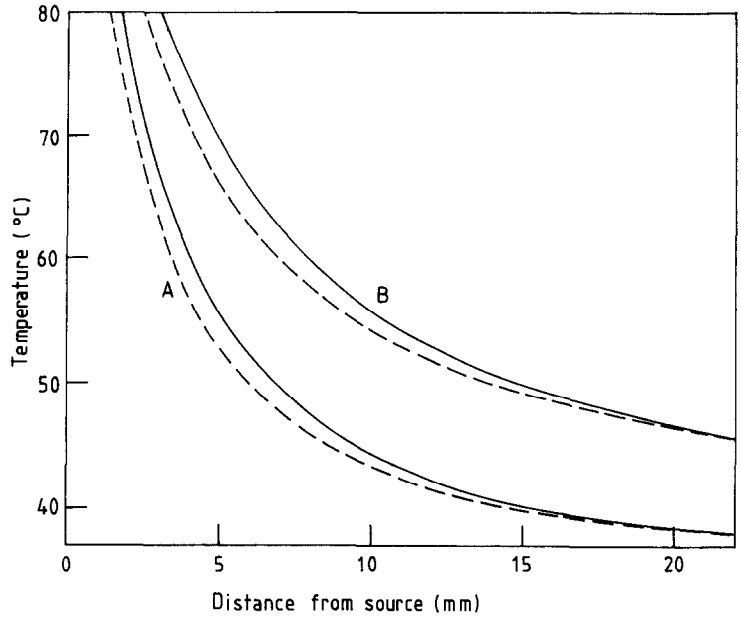

FIG. 1. Equilibrium temperature distribution as function of distance from the fibre tip for a spherically symmetric point source for a power of 1.5 W with $k_a = 1.3\ \text{cm}^{-1}$ and $g = 0.8$. The solid lines correspond to $k_s = 9.7\ \text{cm}^{-1}$ and the broken lines to $k_s = 0\ \text{cm}^{-1}$: A: $k_q = 1\ \text{cm}^{-1}$; B: $k_q = 0\ \text{cm}^{-1}$.

to a condition in which there is no perfusion. A laser power of 1.5 W has been assumed although the diagram need only be linearly rescaled on the vertical axis to find the effect of different powers. As can be seen, a perfusion rate such as this, which is appropriate for the rather high values to be found in the liver, makes a substantial difference to the temperature distribution and cannot be ignored here; the same is not necessarily true in, say, the breast where perfusion rates are much lower.

The solid curves in each case give the temperature at a distance r from the tip of the fibre for the cone when $k_s = 9.6\ \text{cm}^{-1}$, $k_a = 1.3\ \text{cm}^{-1}$, and $g = 0.8$. The broken curves are calculated for the same value of k_a but with k_s set equal to zero. Even though there is substantial scattering in the first case it only affects the temperature by a few degrees even quite close to the fibre tip. The case when scattering is ignored corresponds to incident radiation which is absorbed according to the divergent version of Beer's Law. The difference, however, is not really small enough to justify the complete neglect of scattering except perhaps on very long exposures where thermal damage reaches out to a region where most of the energy is in any case transferred by thermal conduction rather than electromagnetic radiation.

2. Method of Solution

Equations (1) to (3) were solved using the method of lines. The method of lines is essentially a technique for replacing a system of partial differential equations in two or more independent variables by an approximate system of ordinary differential equations in one of these variables, in this case the time variable. See Jones, Smith, and Klunker [11]. The method of lines has a number of advantages over other algorithms. It can be used to solve every type of partial differential equation whether elliptic, parabolic, or hyperbolic, as well as ordinary differential equations other than those of eigenvalue type. It is very suitable for the study of the evolution of such a system as this. The final equilibrium solution is not required; what is of interest is the way the system varies with time so that the surgeon can know when the tumour has been treated. He can then turn the laser off so that no damage is done to healthy tissue surrounding it. Numerical solution is necessary since there is no analytical solution which distinguishes between living and dead tissue or which can make allowance for spherically asymmetrical output of intensity from the tips of the fibres. Nor could analytical methods easily cope with variations of the physical parameters with temperature. Matthewson [2] found such variations, and Wilson and Patterson [12] reported that substantial variations can occur on the death of tissue.

The resulting set of ordinary differential equations generated by the method is integrated by the initial value Gear–Hindmarsh algorithm—i.e., the Gear backward

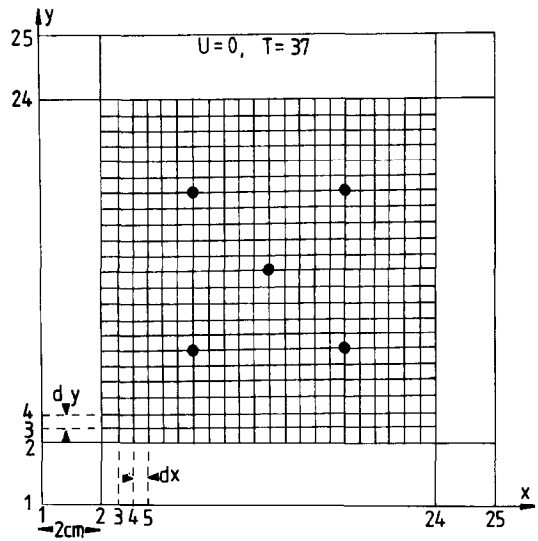

FIG. 2. The grid employed for the computations in the x, y plane for given z. The solid circles indicate the axes of the fibres. On the boundaries (the grid points for which either coordinate is numbered 1 or 25), U has the value 0, and T has the value 37°. The values dx and dy are both 3/22 cm; the value of dz is 0.25 cm.

differentiation formulae for stiff equations [13, 14]. In the integration algorithm the Jacobian matrix is assumed to be banded, which is normally the case in the method of lines and is calculated by finite differences. Interpolation is performed to reach the end of the time step intervals. The derivatives were approximated by 5-point Lagrangian differentiation formulae on a nonlinear grid. The boundary conditions at infinity are replaced by the condition applied at the edges of the grid. A nonlinear grid system of $x: 25 \times y: 25 \times z: 15$ was used; the x, y plane is shown in Fig. 2.

With a grid system of size $25 \times 25 \times 15$ the method of lines approximation produces a system of 9375 ordinary differential equations. But as the solutions are known at the boundaries this set of ordinary differential equations reduces to a system of 6877 equations. In effect the boundary points are evaluated algebraically rather than by numerical integration, and this suppresses error waves from starting at the boundary points.

The complete problem was programmed in FORTRAN 77 [15] and the resulting code was run on a DEC System 10 based on two KL10 processors. The light intensity equation and the temperature equation were solved separately, as the power density equation reaches the steady state very rapidly compared with the temperature equation. If they were solved together the integration step size would have to be a very small value to obtain a stable solution, therefore it would require a large amount of CPU time. The CPU times to solve the equations separately to the given relative tolerance of 10^{-4} were 2 h 8 min for the power density equation and 2 h 36 min for the temperature equation for t in the range from 0 to 100 s.

In the method of lines the accuracy is governed by the number of spatial divisions, the order of the spatial coupling, and the truncation error of the integration algorithm. The first two dominate the overall error control in the method, and the integration algorithm adjusts the integration step size so that the local truncation error of each variable is below a specified maximum. This error is the local error at each integration step, and they can accumulate over a number of steps to cause a large global error. However, in a stable algorithm they tend to cancel rather than accumulate, so the global error does not grow at an unacceptable rate. The latter also depends on the equation set being solved.

A simple check for stability and error control was carried out by changing the derivative approximations from 5- to 3-point Lagrangian differentiation formulae, but still using the relative integrator tolerance of 10^{-4}. The results obtained by this exercise only showed a difference in the 4th/5th decimal place, and the CPU time for the 3-point method reduced to 1 h 13 min for the power density equation and 1 h 49 min for the temperature equation.

The boundary conditions were applied to the system after the derivatives had been discretised, as this produced a more stable set of ordinary differential equations. In both cases (3-point and 5-point) in the death condition, Eq. (3), the integral was solved using a 32-point Gaussian quadrature formula. The effect of imposing the boundary conditions at a distance of the order of 3 cm from the fibre tips rather than at a theoretically infinite distance has been investigated and found

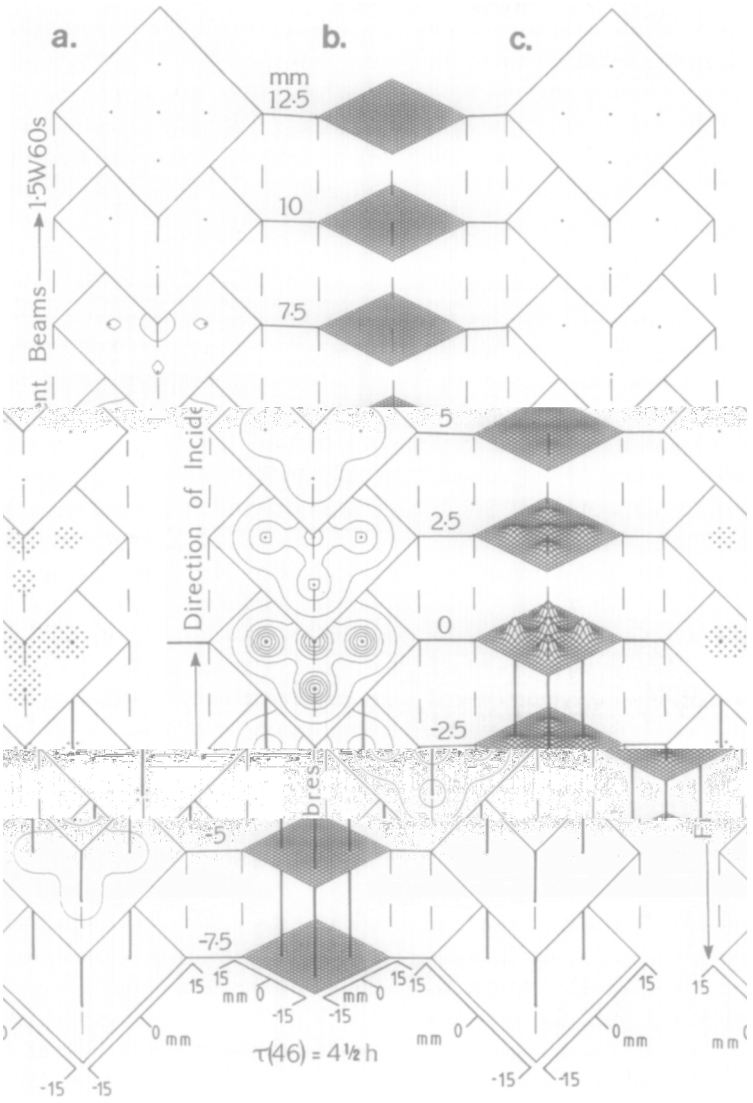

FIG. 3. Temperature profiles and zone of necrosis in planes perpendicular to the axes of the fibres for Case 1 with a power 1.5 W per fibre after 60 s. The distance between the planes is 2.5 mm, the fibres at adjacent corners of the square are 13.4 mm apart, and the fourth plane from the bottom of the [illegible] perspective in (b). The zone of necrosis is shown in (c). The obscured quarter of each of the lower planes in (a) and (c) is the same as the other three quarters.

not to affect the solution. Overall, the errors in the solutions were approximately given by $1/N^2$, where N is the number of grid points defining the discretisation. In the drawing of the surface and contour diagrams, as in Fig. 3, for example, a taut cubic piecewise polynomial, the "ratio slope" method, was used [16] so that no extraneous turning points are created near the boundaries. Such a piecewise polynomial could easily be used to approximate the derivatives in the method of lines instead of Lagrangian differentiation formulae; this would be particularly appropriate in the case of a highly irregular grid.

3. Discussion

The program has been run with a number of different sets of values for the physical parameters of tissue. In all cases the specific heat and density of tissue were taken equal to those of water, and the values for blood were taken as $3.217\,\mathrm{J\,g^{-1}\,°C^{-1}}$ and $1.0983\,\mathrm{g\,cm^{-3}}$, respectively. In all cases the fibres were arranged in the pattern of a square of side 1.34 cm with an extra fibre at the centre. Two examples are given in detail here.

Case 1 is an example of isotropic scattering so that $g=0$ with a laser power of 1.5 W per fibre and a value for α of 30°. A value for the perfusion rate q of $6.37\times10^{-4}\,\mathrm{s^{-1}}$ was adopted which is reasonable for breast tissue but perhaps rather low for the liver [17, 18]; in the case of the liver, however, it is possible to cut off the blood supply entirely during treatment if so desired. The values taken initially for k_a and k_s were both $3\,\mathrm{cm^{-1}}$. The values used are appropriate to blood thrombus [19]; it should be noticed that the absorption coefficient k_a employed here, consistently with Ishimaru's definition, has half the value of the more usually quoted coefficient that assumes a model of absorption of the Kubelka–Munk type. See reference [4, Chaps. 7 and 10]. The value used for $\tau(46)$ is 4.5 h; in their paper on the modelling of laser treatment of a port-wine stain, van Gemert, de Klein, and Hulsberger-Henning [20] suggest a value for $\tau(60)$ of 1 s, which is equivalent.

Case 2 is an attempt to model the treatment of the liver by a Nd: YAG laser with an exposure time of 1 min, with a laser power of 1 W per fibre. The value of α is 5°. A blood perfusion rate of $q=22\times10^{-4}\,\mathrm{s^{-1}}$ has been used. Values for k_a and k_s have been based on the $11\,\mathrm{cm^{-1}}$ for liver reported by Wilson and Patterson [14] for k_t at 0.63 μm wavelength, in the absence of data for 1.06 μm. The values of k_a and k_0 were then chosen to obtain as good agreement as possible with the observations reported by Matthewson *et al.* [2] using the analytic solutions given above. This led to values for k_a of $1.3\,\mathrm{cm^{-1}}$ and of 0.8 for g; recent results obtained by Jacques and Prahl [21], Yoon *et al.* [22], and Wilson and Patterson [14] all indicate that tissue is strongly forward scattering, and the value used here for g is compatible with their results. Van Gemert *et al.* [23] has shown that the diffusion approximation is not entirely satisfactory when g is greater than about 0.9, but the value used here avoids that problem.

For Case 1 the results obtained are shown in Fig. 3. The three columns in the

figure show contours of temperature in 10° steps from 40°, graphs of the temperature, and the necrotic zone in planes perpendicular to the fibres at a separation of 2.5 mm. It will be seen that the necrotic zone consists of five overlapping, roughly spherical regions in the form of a cross. For these values of the constants, either the exposure is too short or else the separation of the fibres is too great to obtain a

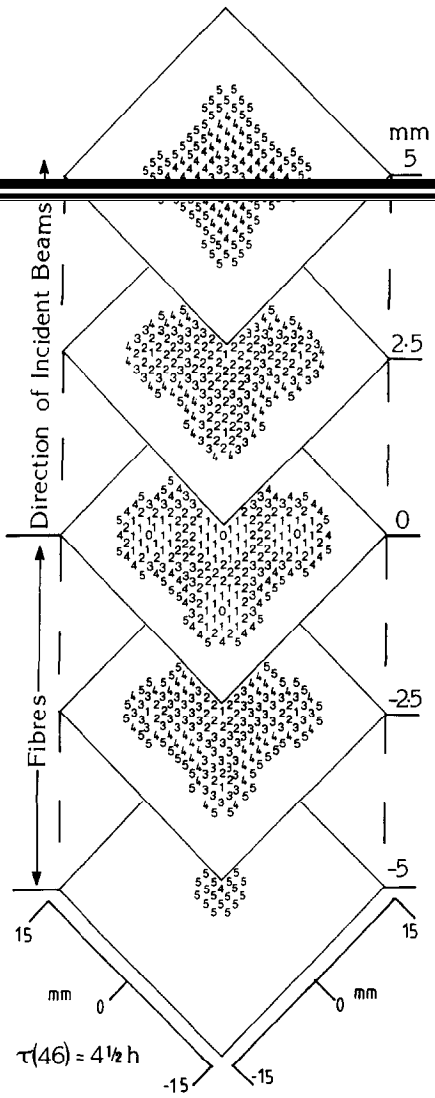

FIG. 4. The region of necrosis for a power of 1 W at 1-min intervals, shown as in Fig. 3c. The figures indicate the number of minutes at which tissue at the corresponding grid point was first recorded as dead.

more smoothly shaped necrotic zone. That could also be obtained in theory by increasing the laser power, but the power used in this example is very much the maximum possible in practice without charring.

The effect of using a lower power for a longer period of time was then investigated. With a power of 1 W per fibre, a total exposure of 5 min was simulated, and the size of the necrotic zone recorded after 1, 2, 3, 4, and 5 min. The result is shown in Fig. 4. The numbers plotted show the number of minutes after the start of treatment at which the tissue at each grid-point is first recorded as dead. It can be seen that initially the tip of each fibre is the centre of an expanding zone separate from the others, but that after 3–4 min, the zone becomes a fairly smoothly shaped single region expanding as if from the centre of the square. Even after 5 min the necrotic zone had not reached as far as 7.5 mm from the plane of the fibre tips. From this calculation it is possible to obtain the mean diameter of the necrotic zone, here defined as the diameter of the sphere with the same value, as a function of exposure time. The result is shown in Fig. 5 and exhibits a very strong qualitative similarity to Fig. 2 of Matthewson's paper [2] in the case of the three lowest powers shown there. This is encouraging support for the underlying principles of the model.

Figure 6 shows the results for Case 2 in the same way as in Fig. 3. The necrotic zone is rather similar in form to Case 1; the power of 1 W leads to lower temperatures at the fibre tips. The maximum temperature in this case is just under 100 °C, whereas with 1.5 W higher temperatures occur and lead to charring. To treat a more smoothly shaped region without excessive temperatures, a longer time can be employed or the fibres can be placed closer together. Notice that in this

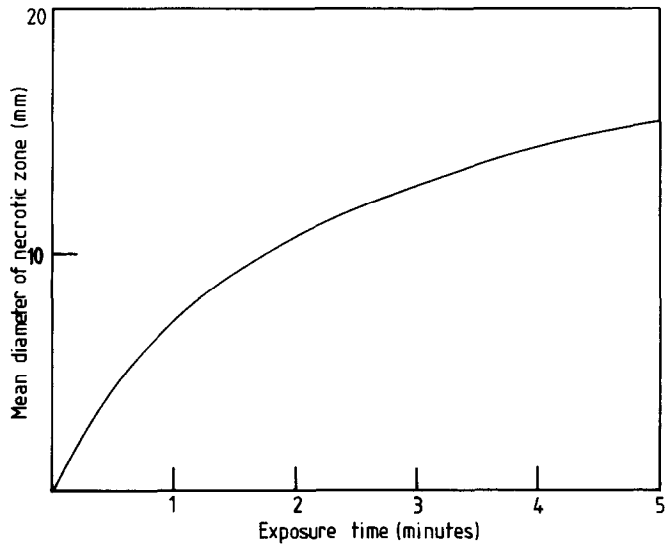

FIG. 5. The mean diameter of the necrotic zone as a function of exposure time for the same calculation as in Fig. 4.

example, as in the first example, there is a detectable asymmetry between the region ahead of the fibre tips, and the region behind them. The difference, however, is really not very great, and suggests that information obtained from spherically symmetric mathematical models of the intensity distribution at the fibre tips can give useful information.

It has been possible to write a program which solves the equations of a mathematical model of the treatment of tumours by hyperthermia, using a cluster of

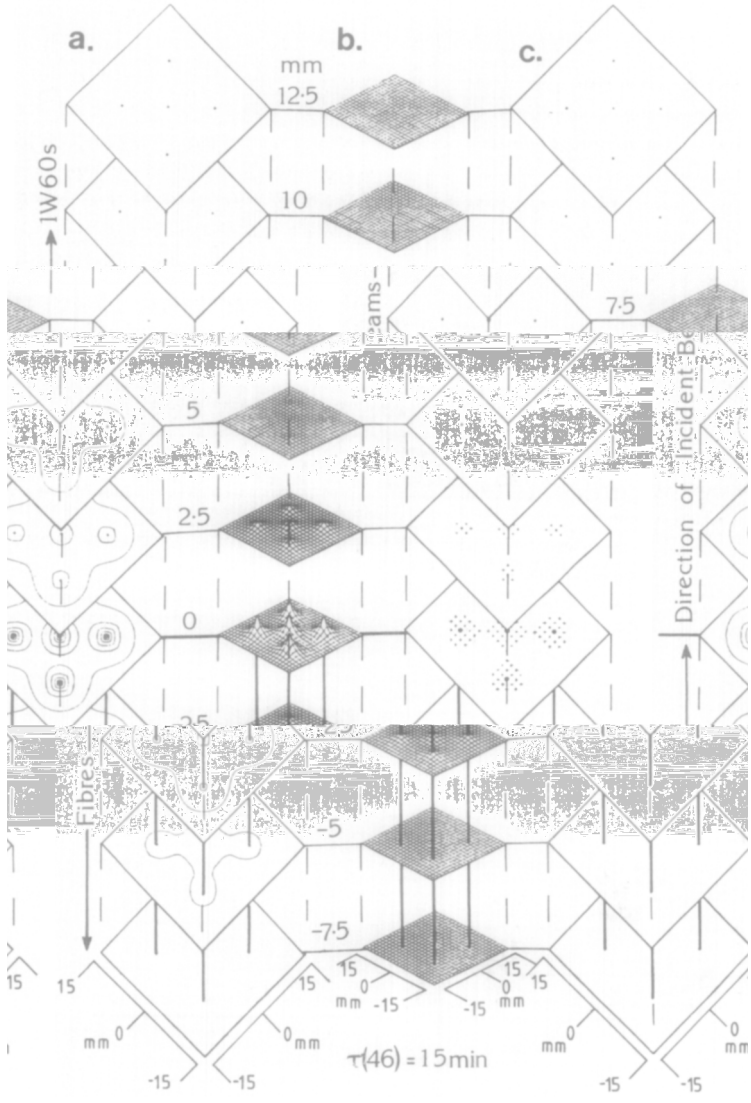

FIG. 6. Temperature profiles and zone of necrosis for Case 2, shown in the same way as for Fig. 3.

fibres. The model can be used to obtain insight into the shape of the region treated and the effects of taking different values for parameters of the problem, some of which are not yet too well known. With better values, programs such as this could become a valuable aid to the surgeon in determining the nature of the most appropriate treatment of specific tumours.

REFERENCES

1. S. G. BOWN, *World J. Surgery* **7**, 719 (1983).
2. K. MATTHEWSON, P. COLERIDGE-SMITH, J. P. O'SULLIVAN, T. C. NORTHFIELD, AND S. G. BROWN, *Gastroenterology* **93**, 550 (1987).
3. H. FUJI, T. ASAKURA, S. JUTAMULIA, S. KANEKO, AND M. TSURU, *Opt. Laser Technol.* **16**, 40 (1984).
4. A. ISHIMARU, *Wave Propagation and Scattering in Random Media*, (Academic Press, New York, 1978), Vol. 1.
5. R. A. J. GROENHUIS, H. A. FERWEDA, AND J. J. TEN BOSCH, *Appl. Opt.* **22**, 2456 (1983).
6. J. W. HAND, J. L. LEDDA, AND N. T. S. EVANS, *Phys. Med. Biol.* **27**, 1 (1982).
7. J. A. DICKSON AND S. K. CALDERWOOD, *Ann. N.Y. Acad. Sci.* **335**, 180 (1980).
8. J. M. DOWDEN, M. P. DAVIS, P. KAPADIA, AND K. MATTHEWSON, *Lasers Med. Sci.* **2**, 211 (1987).
9. A. J. WELCH, *IEEE J. Quant. Elec.* **QE-20**, 1471 (1984).
10. M. ABRAMOWITZ AND I. A. STEGUN, *Handbook of Mathematical Functions* (Dover, New York, 1965), Chap. 5.
11. D. J. JONES, J. C. SOUTH, AND E. B. KLUNKER, *J. Comput. Phys.* **9**, 496 (1972).
12. B. C. WILSON AND M. S. PATTERSON, *Phys. Med. Biol.* **31**, 327 (1986).
13. C. W. GEAR, *Numerical Initial Value Problems in Ordinary Differential Equations* (Prentice-Hall, Englewood Cliffs, NJ, 1971).
14. A. C. HINDMARSH, URCL-30059, Lawrence Livermore Laboratory, Livermore, CA, 1973 (unpublished).
15. DIGITAL EQUIPMENT CORPORATION, *DEC System 10: FORTRAN Programmer's Reference Manual* (Maynard, MA, 1982).
16. M. P. DAVIS AND J. M. DOWDEN, *Computing* **38**, 299 (1987).
17. J. PATTERSON AND R. STRANG, *Int. J. Radiat. Oncol. Biol. Phys.* **5**, 235 (1979).
18. U. PLENGVANIT *et al.*, *Austr. N. Z. J. Med.* **1**, 44 (1972).
19. M. J. C. VAN GEMERT, G. A. C. M. SCHETS, E. M. STASSEN, AND J. J. BONNIER, *Lasers Surg. Med.* **5**, 219 (1985).
20. M. J. C. VAN GEMERT, W. J. A. DE KLEIN, AND J. P. HULSBERGER-HENNING, *Phys. Med. Biol.* **27**, 1089 (1982).
21. S. JACQUES AND S. PRAHL, *Lasers Surg. Med.* **6**, 494 (1987).
22. G. YOON, A. J. WELCH, M. MOTAMEDI, AND M. J. C. VAN GEMERT, *IEEE J. Quant. Elec.* **QE-23**, 1721 (1987).
23. M. J. C. VAN GEMERT, A. J. WELCH, W. M. STAR, M. MOTAMEDI, AND W.-F. CHEONG, *Lasers Med. Sci.* **2**, 295 (1987).